

Deformation mechanism and texture and microstructure evolution during high-speed rolling of AZ31B Mg sheets

Hualong Li · Emilie Hsu · Jerzy Szpunar · Hiroshi Utsunomiya · Tetsuo Sakai

Received: 14 April 2008 / Accepted: 26 September 2008 / Published online: 23 October 2008
© Springer Science+Business Media, LLC 2008

Abstract High-speed rolling of AZ31B was carried out under various preheating temperatures from RT to 350 °C. The evolution of texture, grain sizes, and dislocation density distribution (Kernel average misorientation distributions) in the mid-thickness and surface layer were investigated. Computer simulations of deformation textures were also performed in order to understand deformation mechanisms. It is concluded that the temperature increase due to the plastic and frictional working during high-speed rolling makes the $\langle c+a \rangle$ slip system more active and, hence, improves the ductility. The surface layer of the specimen has higher temperature and experiences severe shear stress; therefore the texture, microstructure, and dislocation density distribution are different from those of the mid-thickness of the specimen. Both mid-thickness and surface layer are dynamically recrystallized during the high-speed rolling.

Introduction

Magnesium and its alloys have a large potential for applications in automotive industry. Compared with steels and aluminium alloys, magnesium alloys are lighter and the weight reduction can be linked to lower fuel consumption and lower green gas emission.

Nowadays, the applications of magnesium in casting of automobile parts are already well established. The good castability of magnesium and its alloys allows the production of components that require reasonable mechanical properties but, in many cases, they lack other desired properties [1, 2].

Even higher potential for application which is not readily explored until today is associated with wrought magnesium alloys. Generally, wrought magnesium components exhibit a better quality and microstructural homogeneity than their cast counterparts [2]. Although the technology for processing of magnesium sheets and profiles is in existence for more than 60 years [3], no large-volume components are manufactured at present. Due to its hexagonal crystal structure, magnesium has poor ductility at room temperature. At present, the hot-rolling process is a multi-pass operation that still needs improvement to increase productivity and produce materials with the required properties [4].

High-speed rolling was proposed by Sakai and Utsunomiya for fabrication of AZ31B [5] magnesium sheet. During this rolling process, heat is generated by plastic deformation and friction between the material and the rolls and, subsequently, conducted from the materials to cold rolls. By increasing the rolling speed, the duration of contact between the material and the rolls becomes shorter. This results in the rise of the temperature of the sheet material during rolling and, hence, the formation of cracks that result from low-temperature brittleness can be suppressed. Furthermore, higher strain rate deformation at lower temperature suggests that the Zener-Holloman parameter becomes higher, which promotes grain refinement by dynamic recrystallization and can be linked to improvement of the sheet ductility [5].

It is known that the formability of magnesium sheets is closely related to microstructure and texture. Small grain

H. Li · E. Hsu · J. Szpunar (✉)
Department of Materials Engineering, McGill University,
Montreal, Canada H3A 2B2
e-mail: jerzy.szpunar@mcgill.ca

H. Utsunomiya · T. Sakai
Division of Materials and Manufacturing Science, Graduate
School of Engineering, Osaka University, Suita 565-0871, Japan

size [6] and weak {0002} basal plane texture [7] will enhance the formability of the sheets. This article discusses texture and microstructural transformation in AZ31B alloy sheet rolled under different high-speed rolling conditions.

Experimental procedures

Materials of study

The material of study was a commercial AZ31B (Mg–3%Al–1%Zn–0.4%Mn) annealed sheet supplied by Magnesium Elektron North America Inc. The sheet was 2.5 mm thick with a recrystallized microstructure and mean grain size of 8.4 μm at the surface and 12 μm at mid-thickness [8]. The sheet was cold rolled at the speed of 2000 m/min without lubrication. Prior to the rolling, specimen was held for 15 min at 100, 200, and 350 °C in an electric tube furnace, then cold rolled with a reduction of 60% in one single pass. High-speed rolling of specimens without preheating was also performed for a reduction of up to 30%. Further reduction was not possible due to extensive cracking. The specimens were water quenched immediately after rolling. Detailed specifications of the rolling mill and the rolling process can be found elsewhere [5, 9, 10].

Sample preparation for metallographic analysis

The specimens for X-ray diffraction examination were prepared by grinding with SiC papers of up to 1200 grit, and then polishing with diamond pastes of grades 3 and 1 μm . Crystallographic texture measurements were carried out using Siemens D-500 X-ray diffractometer equipped with texture goniometer using Mo radiation. The (0002), (1 $\bar{1}$ 00), and (10 $\bar{1}$ 1) pole figures were collected in the reflection mode on a 5° grid up to 80° sample tilt. The data were analyzed using the TexTools software to calculate orientation distribution functions and recalculate the pole figures.

The sample preparation for electron backscattered diffraction (EBSD) measurement is difficult and a good surface finishing is crucial. Sample preparation consisted of grinding until 1200 grit, polishing with alcohol based diamond suspensions of up to 1 μm and then with colloidal silica slurry for 60 s, and finishing with chemical polishing solution comprising of 10 mL HNO₃, 30 mL acetic acid, 40 mL H₂O, and 120 mL ethanol for 30 s. Local texture was examined using the orientation imaging microscopy (OIM). The system used consists of Philips XL30 S FEG scanning electron microscope (SEM) equipped with EBSD. The scanned data were analyzed using the TSL OIM software.

Results and discussion

Microstructure evolution

Microstructure examination of the specimens was performed using orientation imaging microscopy (OIM). OIM also enables us to perform the grain boundary and crystallographic orientation examination by analyzing the electron backscattered patterns (EBSP) collected on the specimens.

Figure 1 shows the surface and mid-thickness microstructures of the high-speed rolled specimens preheated at various temperatures. Different colors in the microstructures represent different grain orientations that are defined according to the color-orientation map in an inverse pole figure space.

Figure 1a and b shows the mid-thickness and surface microstructures of the high speed rolled specimens without preheating. In both microstructures large grains and small equiaxed grains were observed. It is believed that the large grains are deformed grains while the small equiaxed grains are dynamically recrystallized. During the high-speed rolling, the specimen temperature can rise due to large amount of the plastic and frictional work generated in very short time [9, 10]. It is possible that the temperature can rise to such a level that it can cause recrystallization. This is supported by microstructures presented in Fig. 1. Figure 1c–h presents the rolled microstructures preheated at different temperatures, 100–350 °C. Because these specimens were preheated at higher temperatures, the actual temperatures of the specimens during high-speed rolling were also higher compared to that of the specimen without preheating and the corresponding microstructures were, therefore, more readily recrystallized. This is evident in Fig. 1c–h where the microstructures have only equiaxed grains.

It is also worthwhile to notice the grain size differences between the surface and mid-thickness microstructures shown in Table 1. When the preheating temperature was lower than or equal to 200 °C, the recrystallized grains had slightly smaller grain size in the surface layer than in the mid-thickness layer. This is due to the higher shear stress in the surface layer. During the rolling process, the surface layer of a specimen experiences shear stress whereas the center layer does not. The shear stress generates higher stored energy in the surface layer. During recrystallization process, high stored energy facilitates the nucleation of recrystallized grains and the density of recrystallized nuclei is high. High density of nuclei leads to small recrystallized grains.

The grain size distribution was different when the specimens were preheated at 350 °C. As shown in Fig. 1g and h, the surface layer had a slightly larger grains size

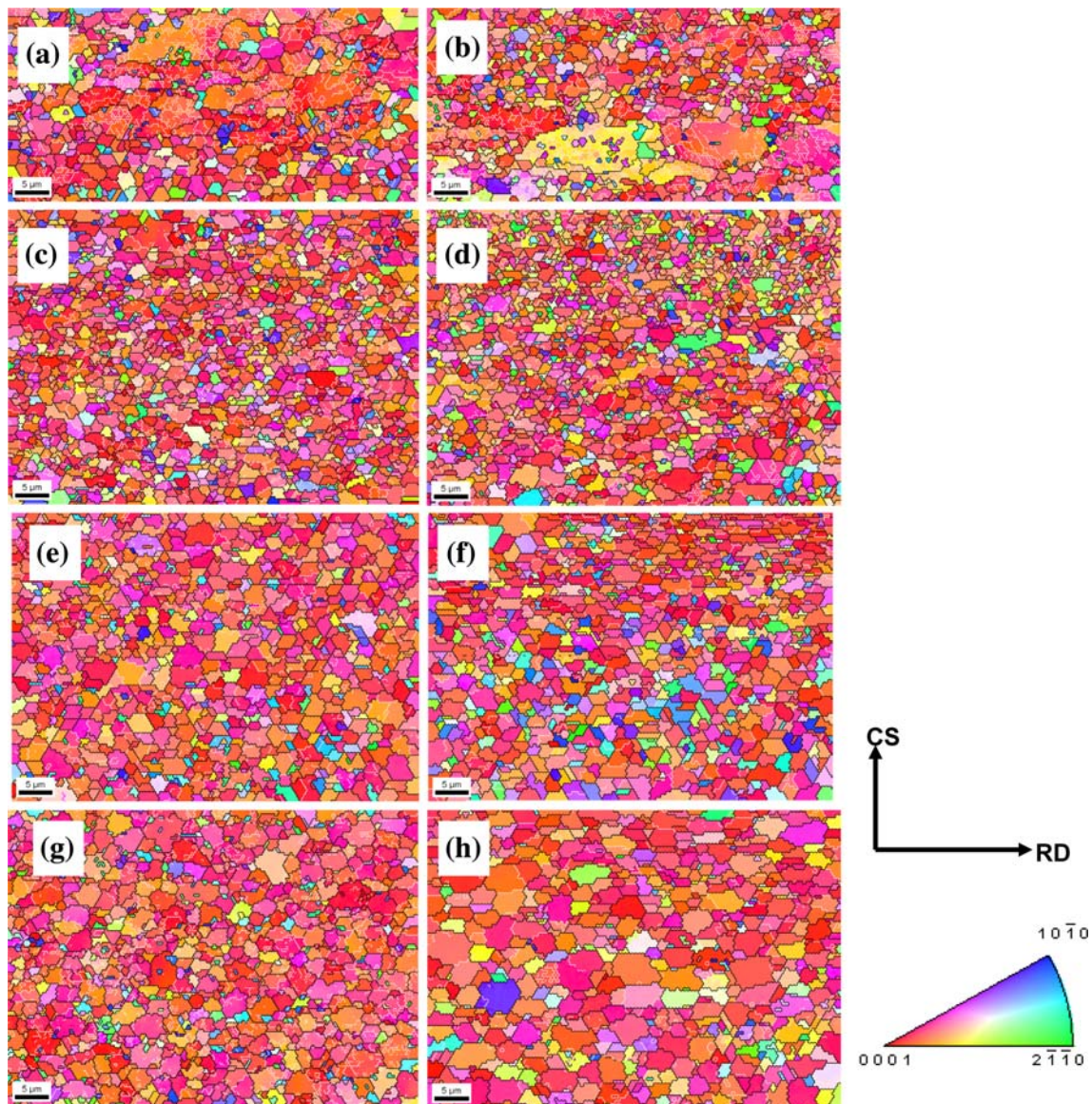


Fig. 1 OIM cold-rolled microstructures of the specimens preheated at various temperatures, color coded by crystallographic orientations: **a** mid-thickness without preheating, **b** surface without preheating, **c** mid-thickness preheated at 100 °C, **d** surface preheated at 100 °C, **e**

mid-thickness preheated at 200 °C, **f** surface preheated at 200 °C, **g** mid-thickness preheated at 350 °C, and **h** surface preheated at 350 °C (CS = ND)

Table 1 Mean grain sizes in the rolled specimens at regions beneath the surface and at mid-thickness

Rolling temperature (°C)	Mean grain size (μm)	
	Mid-thickness	Surface
RT	2	3
100	2	2
200	2	2
350	3	4

than that of the mid-thickness layer. This phenomenon may be caused by grain growth in the surface layer. During high-speed rolling, the surface temperature is

higher than that of the middle layer. To verify this, the temperatures at the surface and center layers of the specimens were estimated from the heat balance. It was clear from the measurements that the surface temperature was higher than that at the center. When preheated at 350 °C, the surface temperature of the specimen during high-speed rolling was even higher. It is speculated that the high temperature in the surface layer caused not only recrystallization, but also grain growth. Therefore, the grain size in the surface layer is larger than that of the mid-thickness region. The grain growth process in Fig. 1a–g might not be significant due to the lower preheating temperature.

Overall, the experimental results in Fig. 1 suggest dynamically recrystallized microstructures during high-speed rolling. In order to further verify this assumption, the Kernel average misorientation distributions of the surface and center layers preheated at all four temperatures were measured and analyzed.

Kernel average misorientation

The Kernel average misorientation distribution is a tool in OIM analysis that can be used as a representation of dislocation density distribution in different grains. As a

general rule, Kernel average misorientation is high ($>1^\circ$) in deformed grains due to the high density of dislocations. In contrast, Kernel average misorientation is low ($<1^\circ$) in recrystallized grains.

The specimens of all rolling conditions were examined for Kernel average misorientation and the results are given in Fig. 2. Here, the blue color shows the lowest dislocation density areas; the green color shows the higher dislocation density areas; and the red color shows the highest dislocation density areas. For specimens without preheating, the results of dislocation densities are given in Fig. 2a and b for the mid-thickness and the surface layer, respectively.

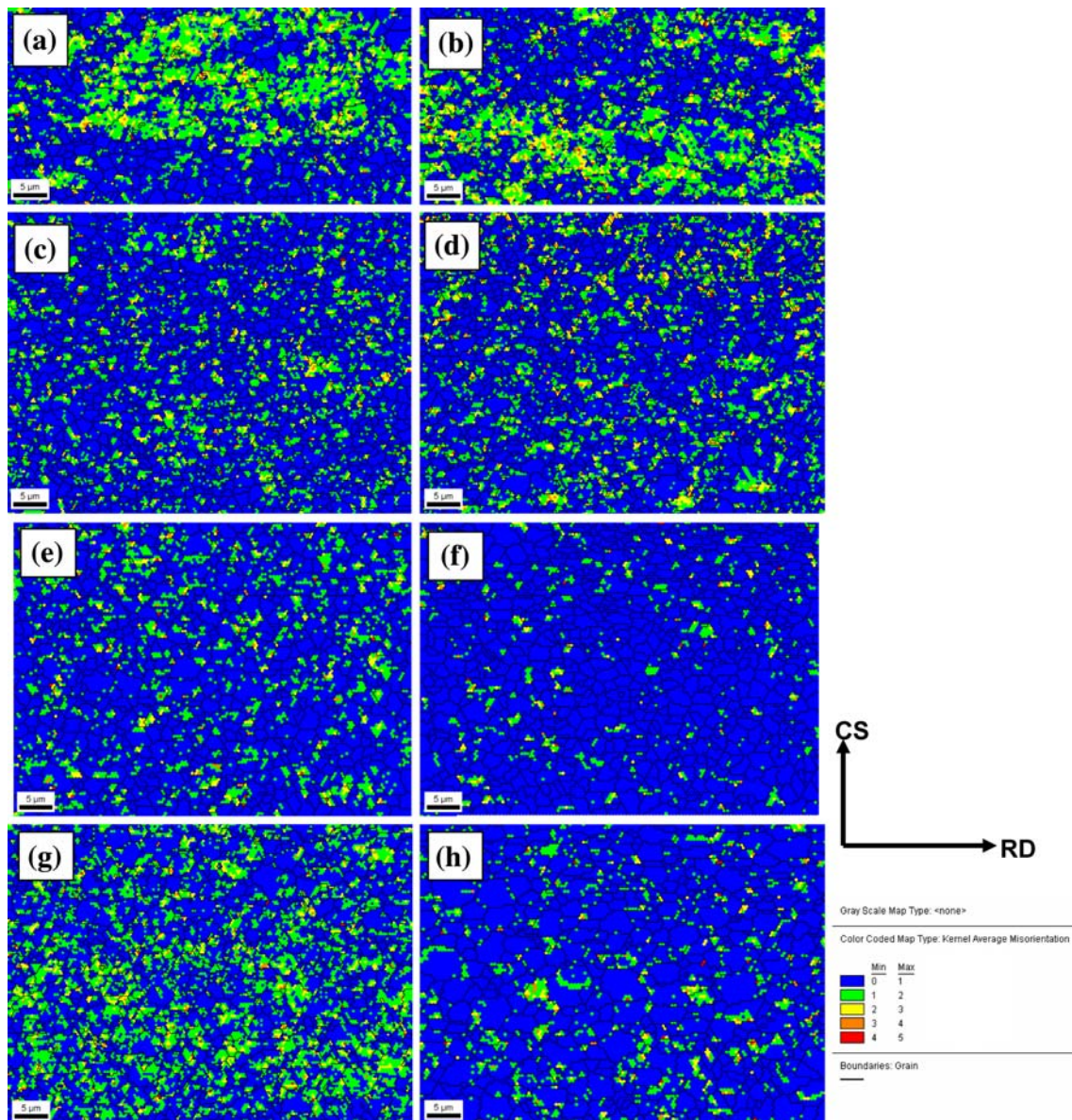


Fig. 2 Kernel average misorientation distribution of the specimens preheated at various temperatures: **a** mid-thickness without preheating, **b** surface without preheating, **c** mid-thickness preheated at

100 °C, **d** surface preheated at 100 °C, **e** mid-thickness preheated at 200 °C, **f** surface preheated at 200 °C, **g** mid-thickness preheated at 350 °C, and **h** surface preheated at 350 °C (CS = ND)

Both of them show that the dislocation densities were not evenly distributed throughout the microstructure. Some areas had high dislocation density as represented by the green and the red colors which indicated the locations of deformed grains. The rest of the microstructure had low dislocation density as represented by the blue color which indicated the locations of recrystallized grains. By comparing Fig. 1a and b with Fig. 2a and b, one can see that the large grains in Fig. 1a and b correspond to the high dislocation density areas in Fig. 2a and b and small grains in Fig. 1a and b correspond to the low dislocation density areas in Fig. 2a and b. This supports the previous observation that the large grains in Fig. 1a and b are deformed while the small grains are recrystallized grains.

From Fig. 2c–h, low dislocation density ($<1^\circ$) was generally observed throughout the microstructures. Such distributions indicate recrystallization or partial recrystallization in the specimens and, are, thus consistent with the results presented in Fig. 1c–h where small equiaxed grains can be found. Therefore, Fig. 2c–h support the previous conclusion of dynamic recrystallization.

It was also observed that the degree of misorientation for all preheating temperatures was lower at the surface region than at the mid-thickness of the sheet. To illustrate such observation, one of the quantitative Kernel average misorientation distributions is shown in Fig. 3 for 350 °C preheated specimen. As can be seen, the maximum of misorientation fraction distributions were at 0.5 and 0.75° for the surface layer and the center layer, respectively. This experimental finding is not what normally is expected in deformed grains. In deformed microstructure, one expects to see higher dislocation density in the surface layer than that of the mid-thickness region, because the surface layer experiences severe deformation due to shear stress. This indicates that the microstructures in Fig. 2c–h are not in deformed state. In fact, they represent recrystallized microstructures. The lower dislocation density in the surface layer is the

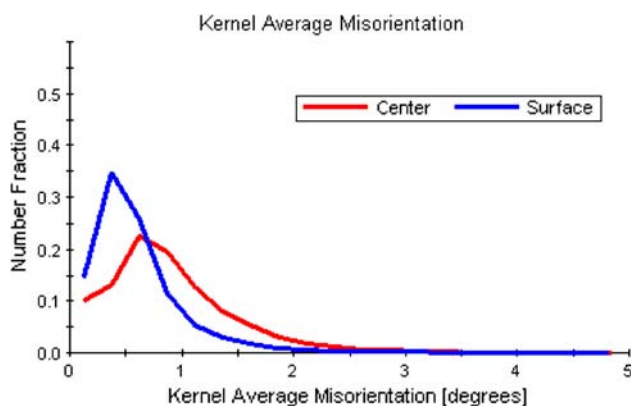


Fig. 3 Kernel average misorientation curves of the rolled specimens at regions beneath the surface and at mid-thickness for the specimen preheated at 350 °C

consequence of the higher temperature in the surface layer that causes more complete recrystallization. Among all cases presented in Fig. 2, Fig. 2h shows the lowest dislocation density which is related to the highest temperature the specimen experienced during the high-speed rolling.

Texture evolution and deformation mechanism

The initial texture of the annealed magnesium AZ31B sheet is shown in Fig. 4. The scale of intensity was normalized so that the value of 1.00 represented the intensity from the specimen with random grain orientation. The (0002) basal pole figure indicates that majority of c -axes of the grains is aligned with the sheet normal direction. Figures 5 and 6 illustrate the crystallographic textures at mid-thickness and beneath the surface layer, respectively, after high-speed rolling with various preheating temperatures. In Fig. 5, the basal poles of the mid-thickness textures split toward the rolling direction and, the magnitude of splitting increased with the increase of the preheating temperature. According to our previous study [11], such a split indicates the activation of $\langle c+a \rangle$ slip system that is $\{01-11\}\langle 2-1-10 \rangle$. The $\langle c+a \rangle$ slip system can only be activated at higher temperatures. The exact temperature to activate $\langle c+a \rangle$ slip system is not well defined and depends on the alloy composition. As it was mentioned already, during high-speed rolling, the specimen temperature can rise due to the plastic and frictional work [9, 10] and, the $\langle c+a \rangle$ system can be activated. Without preheating, it appeared that the heat generated from the high-speed rolling was not enough to activate the $\langle c+a \rangle$ system and, therefore, no split of the basal pole was observed in Fig. 5a. If the $\langle c+a \rangle$ system is not active, the deformation is accommodated by the basal slip and the extension twinning systems only, and the formability is poor [11]. This analysis was supported by the experimental

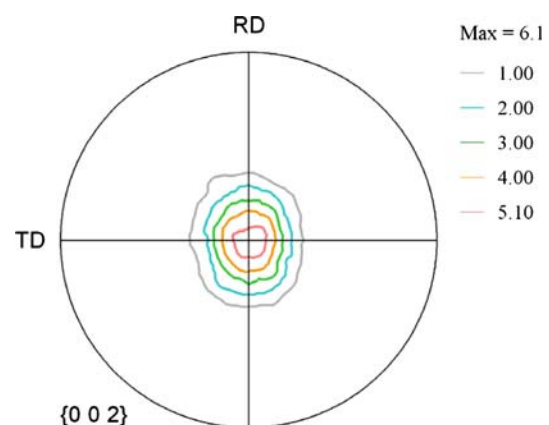


Fig. 4 Initial texture of the mid-thickness of the annealed magnesium AZ31B sheet

Fig. 5 The textures at the mid-thickness at various preheating temperatures: **a** no preheating, **b** 100 °C, **c** 200 °C, and **d** 350 °C

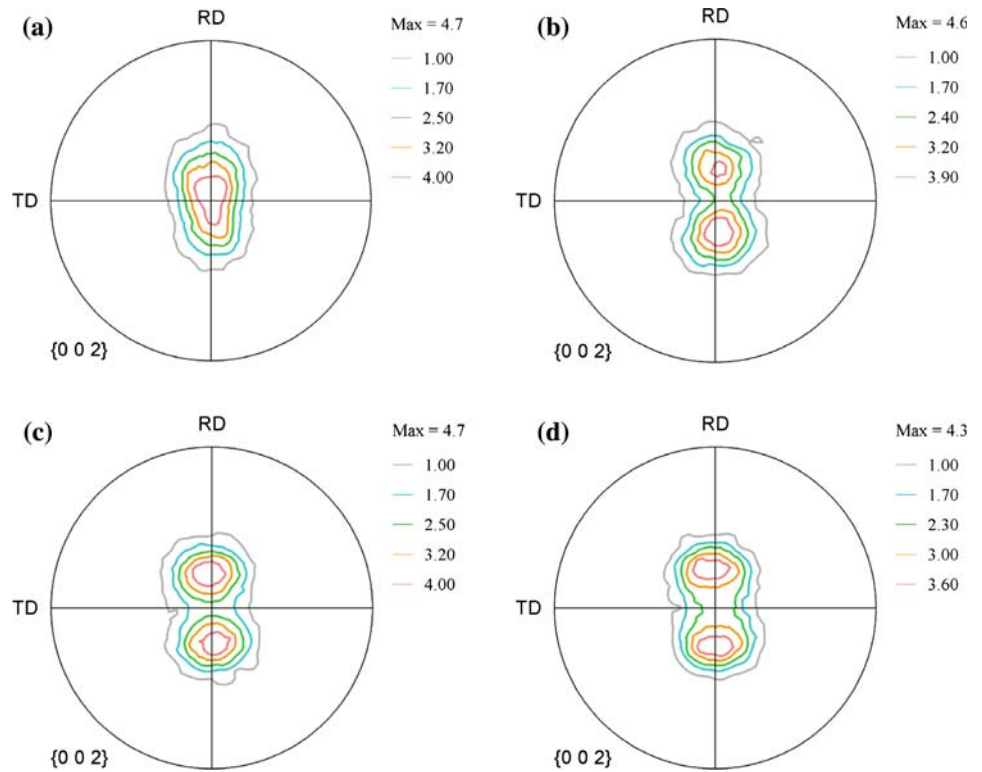
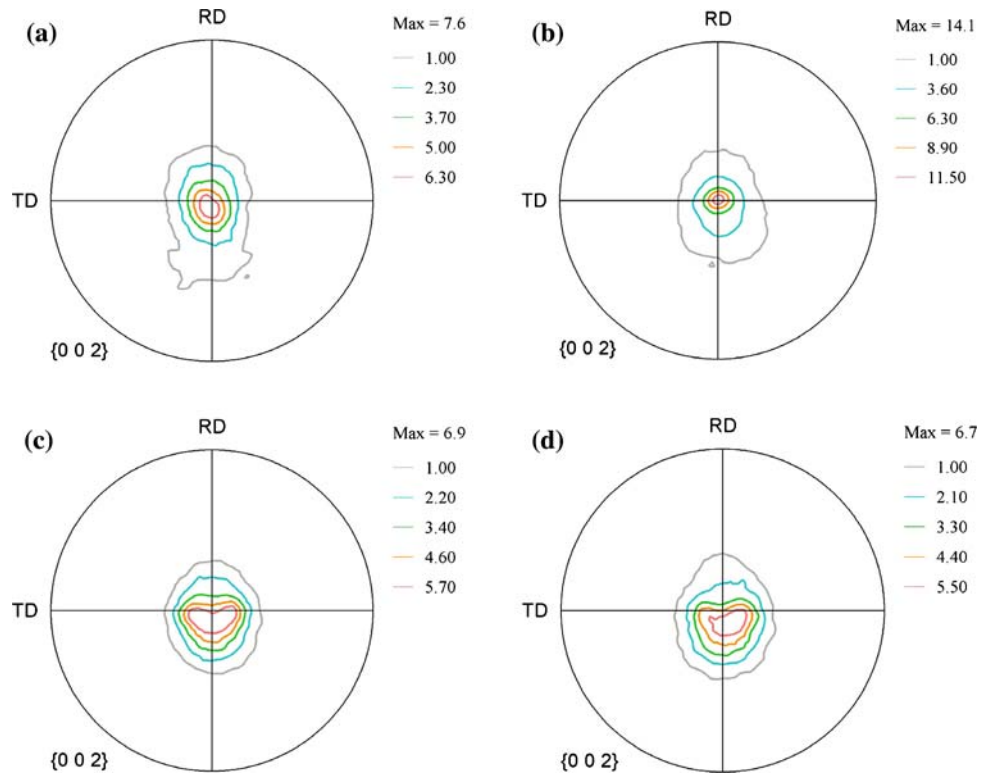


Fig. 6 The textures of surface layers at various preheating temperatures: **a** no preheating, **b** 100 °C, **c** 200 °C, and **d** 350 °C



results showing that the specimen deformed at RT had extensive edge cracking at 30% reduction, whereas all other specimens were rolled up to 60% reduction and had small number of edge cracks.

Figure 6 presents the textures of the surface layer for various preheating temperatures. These regions had the basal textures similar to the initial texture of the annealed material as presented in Fig. 4. However, the basal poles on

the (0002) pole figures were shifted downward along the rolling direction. The magnitude of the shift increased as the preheating temperature increased. It is suspected that the amount of shear strain on the surface layer, which increased with temperature, caused the shift.

To examine the roles of slip systems and shear stress in texture evolution during high-speed rolling, computer simulations were performed. Possible influence of recrystallization on texture development was not directly considered in the simulations, but will be addressed later in this section. The computer simulation was based on the VPSC (Visco Plastic Self-Consistent) model [12]. In this model, the specimen was represented by a number of grains. The orientations of these grains were defined in such a way that they reproduce the initial texture of the specimen. Each grain was treated as an inclusion embedded in an effective medium. The effective medium was represented by the matrix that each grain interacts with. Thus, the grains did not interact with each other directly. Each grain, dependent on its own visco-plastic compliance or stiffness, experienced a strain or stress different from that of the medium.

During the simulation of texture evolution, the $\langle c+a \rangle$ slip system was set active in order to produce the basal pole split on the (0002) pole figure. The relative value of Critical Resolved Shear Stress (CRSS) of basal slip was used as 1 in all simulations at various preheating temperatures. The

relative CRSS value of $\langle c+a \rangle$ slip system can be set to any arbitrary value, but must be higher than 1 due to the fact that $\langle c+a \rangle$ slip system is more difficult to activate than the basal slip system. In addition, the relative CRSS value of $\langle c+a \rangle$ slip must decrease with increasing temperature to reflect the fact that $\langle c+a \rangle$ is more active at higher temperature. In order to determine the relative value of $\langle c+a \rangle$ CRSS and the amount of shear strain on the surface layer, simulations using different $\langle c+a \rangle$ CRSS and shear strain were performed. Each of those simulations produced different deformation textures. By quantitative comparison of the simulated and experimental textures, the relative values of $\langle c+a \rangle$ CRSS at various temperatures and the amount of shear strain on the surface layer were determined and the results are given in Table 2. The simulation of texture evolution without preheating, which has been reported in our previous study [11], is not discussed in this article.

Since the simulation parameters in Table 2 were obtained from the comparison of the simulation and experimental results, the following deformation mechanism derived from the simulation results represented only one possible deformation mechanism. In other words, by accepting the following deformation mechanism, it is possible to obtain simulation results that are in agreement with experiments. This study, however, does not rule out the possibilities of other deformation mechanisms.

The mid-thickness textures at various preheating temperatures simulated using the parameters listed in Table 2 are presented in Fig. 7. The visual agreement between the simulated pole figure in Fig. 7 and the experimental pole figure in Fig. 2 is obvious. The quantitative comparisons between the simulated and experimental textures can be demonstrated by the line scans on the (0002) pole figures from the centers to the edge along RD and this is shown in Fig. 8. In this figure, the basal poles for both simulations and experiments are tilted for about 15, 25, and 30° toward RD for preheating temperatures of 100, 200, and 350 °C, respectively. The agreement between simulations and experiments indicates that high-speed rolling activates the

Table 2 CRSS ratios between the basal and $\langle c+a \rangle$ slips used in the simulations

	100 °C	200 °C	350 °C
Mid-thickness			
CRSS ratio (Basal/ $\langle c+a \rangle$)	1/3	1/1.5	1/1
Shear strain	0	0	0
Surface			
CRSS ratio (Basal/ $\langle c+a \rangle$)	1/1.5	1/1.2	1/1
Shear stress	0.7	0.85	1.1

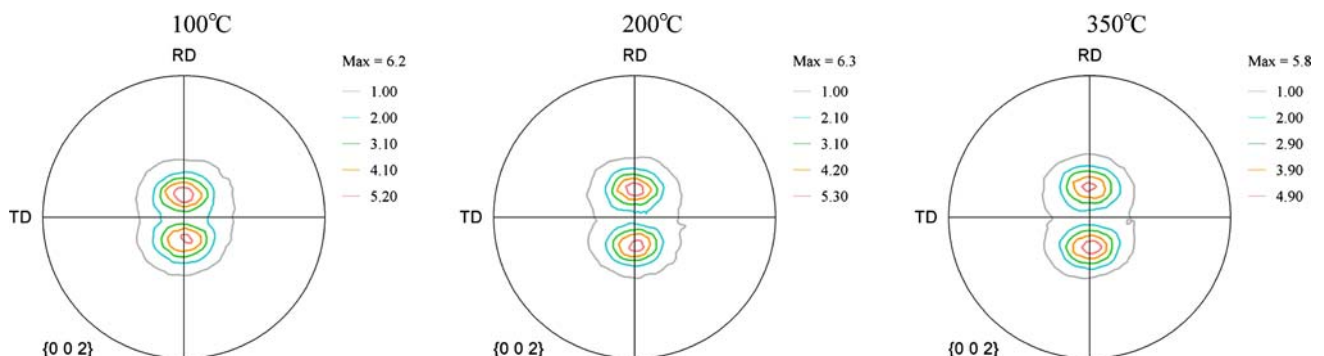


Fig. 7 The textures simulated at the mid-thickness of the sheet rolled to 60% reduction at the given preheating temperatures

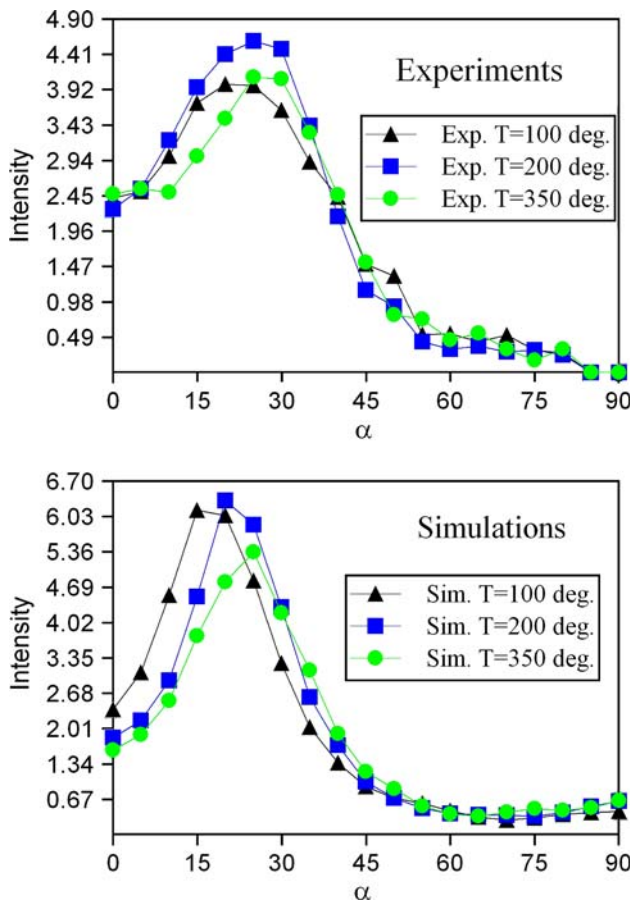


Fig. 8 The comparison of line scans along the rolling direction of the (0002) pole figures from the center to the edge of the pole figure

$\langle c+a \rangle$ slip system because of the elevated temperature generated by the plastic work and the frictional surface forces. The higher the preheat temperature, the more active the $\langle c+a \rangle$ slip is. Contribution of the $\langle c+a \rangle$ slip system to the deformation led to the split of the basal pole and improved the formability of Mg alloy. The simulated contributions of the $\langle c+a \rangle$ slip system to the total deformation at various preheating temperatures are presented in Fig. 9. It can be seen that the $\langle c+a \rangle$ slip system contributed about 20% to the total deformation at preheating temperature of 100 °C, and 60 and 70% for temperatures of 200 and 350 °C, respectively.

For the simulation of texture development in the surface layer, both the slip systems and loading conditions used in the simulations (Table 2) were different from those used for the mid-layer. During high-speed rolling, the surface temperature was higher than that in the mid-thickness. Higher temperature gives rise to more active $\langle c+a \rangle$ slip system. Therefore, the relative CRSS values used in the simulations of surface texture had more active $\langle c+a \rangle$ slip system compared to that of mid-thickness simulation. In addition, the loading condition used in the simulations of

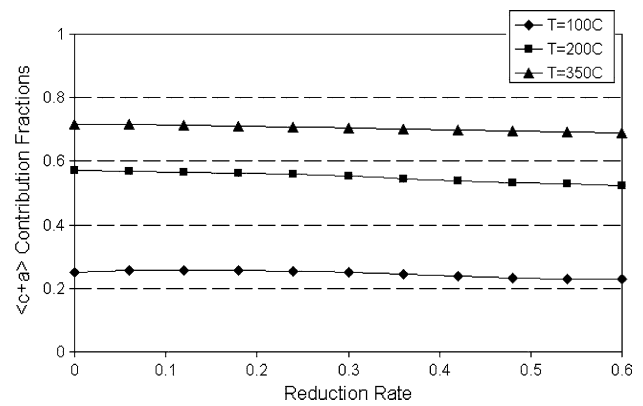


Fig. 9 Contribution of $\langle c+a \rangle$ slip system to the total deformation at various preheating temperatures

the surface layer was also different from that of mid-thickness that had in-plane compression. In the surface layer, there exists shear stress due to the friction between the rolls and the specimen. The higher the temperature, the higher the friction and shear stress are.

The simulated (0002) pole figures are given in Fig. 10. Comparing the pole figures of Figs. 6 and 10, one can see that the simulations agree with the experiments. In both figures, the basal poles were positioned close to the center of the pole figures. This agreement shows that the experimental texture can be reproduced by simulation if the level of active $\langle c+a \rangle$ slip and the amount of the stress is carefully adjusted. It therefore implies that the texture evolution in the surface layer during high-speed rolling is controlled by shear strain and temperature that determine the activities of basal and $\langle c+a \rangle$ slip systems.

However, as discussed earlier, Figs. 1, 2, and 3 demonstrate that the specimens were dynamically recrystallized during high-speed rolling. The experimental textures shown in Figs. 5 and 6 may be considered as textures of dynamic recrystallization. On the other hand, the results representing the simulated deformation texture in Figs. 7 and 10 are in good agreement with the experiments. This implies that the texture does not change during the dynamic recrystallization process and is the same as the deformation texture.

Conclusions

1. The improved formability of AZ31B alloy during high-speed rolling is due to the increase in activation of $\langle c+a \rangle$ slip system that was promoted by the increase of temperature resulted from low dissipation of heat generated during deformation.
2. The texture in the mid-thickness layer is a split basal texture due to the increased activity of $\langle c+a \rangle$ slip system. Increasing the preheat temperature promotes

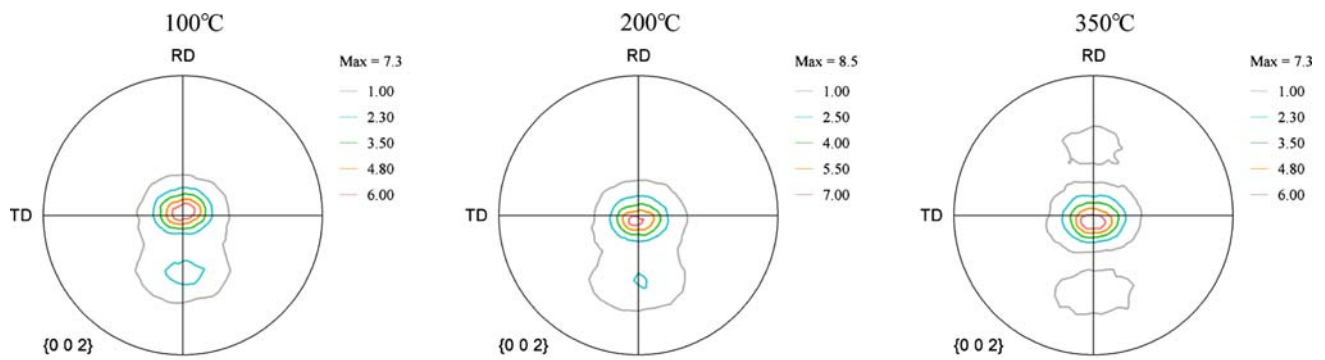


Fig. 10 The simulated textures of the surface layer of the sheet rolled to 60% reduction at various preheating temperatures

the activation of $\langle c+a \rangle$ slip system which increases the basal pole split.

- The surface texture during high-speed rolling is dictated by the shear stress at the surface. High temperature increases the amount of shear strain in the surface layer of the rolled Mg sheet.
- Specimens during high speed rolling are dynamically recrystallized. The texture does not change significantly during dynamic recrystallization and is similar to that of the deformation texture.
- For higher preheating temperatures, when the dynamic recrystallization takes place the grains in both the mid-thickness and surface layers are equiaxed. The grains are smaller in the surface layer than in the mid-thickness location because of the shear stress that promotes the nucleation process of recrystallization. When the preheating temperature is 350 °C, grains in surface layer are larger than in the mid-thickness region due to the higher temperature that promotes grain growth.
- Dislocation density is generally lower in the surface layer than in the mid-thickness area because higher temperature in the surface layer causes more complete recrystallization.

References

- Doerge E et al (2003) Magnesium—alloys and technologies. Wiley-VCM, USA, pp 72–89
- Kainer KU (2003) Magnesium—alloys and technologies. Wiley-VCM, USA, pp 1–22
- Dieringa H et al (2007) In: Beales RS, Luo A, Neelameggham NR, Pekguleryuz MO (eds) Magnesium technology 2007. TMS, Warrendale, pp 3–8
- Friedrich HE, Mordike BL (2006) Magnesium technology. Springer, USA
- Utsunomiya H et al (2006) In: Luo A, Neelameggham NR, Beales RS (eds) Magnesium technology 2006. TMS, Warrendale, pp 201–204
- Koike J, Kobayashi T, Mukai T, Watanabe H, Suzuki M, Maruyama K, Higashi K (2003) Acta Mater 51:2055
- Yoshida Y, Cisar L, Kamado S, Kojima Y (2003) Mater Trans 44:468
- Koh H et al (2007) Mater Trans 48:2023
- Kato K, Saito Y, Sakai T (1984) Trans ISIJ 24:1050
- Sakai T, Saito Y, Hirano K, Kato K (1988) Trans ISIJ 28:1028
- Li H, Hsu E, Szpunar J, Verma R, Carter JT (2007) J Mater Eng Perform 16:321
- Lebensohn RA, Tome CN (1993) Acta Metall 41:2611